DR TYLER JOHN STEVENSON (Orcid ID : 0000-0003-2644-9685)

Article type : Original Article

Running title: Hypothalamic DNA methylation and hamster reproduction

Title: Ovarian hormones induce *de novo* DNA methyltransferase expression in the Siberian hamster suprachiasmatic nucleus.

Authors: Coyle CS[1], Caso F[2], Tolla E[3], Barrett PJ[4], Onishi KG[5], Tello JA[6], Stevenson TJ[3*].

Author Institutions: Department of Physiology, University of Otago, NZ[1]; School of Biological Sciences, University of Aberdeen, Aberdeen UK[2]; Institute of Biodiversity, Animal Health and Comparative Medicine, University of Glasgow, UK[3], Rowett Institute, University of Aberdeen, UK[4]; Department of Psychology, Institute for Mind and Biology, University of Chicago, Chicago USA[5]; School of Medicine, University of St Andrews, UK[6].

Corresponding author:
Tyler Stevenson
Inst. Biodiversity, Animal Health & Comparative Medicine
University of Glasgow
Glasgow, UK
e. tyler.stevenson@glasgow.ac.uk

This article has been accepted for publication and undergone full peer review but has not been through the copyediting, typesetting, pagination and proofreading process, which may lead to differences between this version and the Version of Record. Please cite this article as doi: 10.1111/JNE.12819

Acknowledgements

Brian Prendergast is thanked for helpful comments on a previous version of the manuscript. We thank Eloise Lynch, Dr Sue Barr, Lindsey Duguid, Ana Monteiro and Lynn Stevenson for expert technical assistance. TJS thanks the British Society for Neuroendocrinology and the Society for Reproduction and Fertility for research project funds. PB acknowledges the Scottish Government for funding. The data that support the findings of this study are available from the corresponding author upon reasonable request.

Abstract

Experiments investigated neuroanatomically localized changes in *de novo* DNA methyltransferase expression in the female Siberian hamster (*Phodopus sungorus*). The objectives were to identify the neuroendocrine substrates that exhibit rhythmic *Dnmt3a* and *Dnmt3b* expression across the oestrous cycle and examine the role of ovarian steroids. Hypothalamic *Dnmt3a* expression was observed to significantly increase during the transition from proestrous to oestrous. A single bolus injection of diethylstilbestrol (DES) and progesterone was sufficient to increase Dnmt3a cell numbers and Dnmt3b immunoreactive intensity in the suprachiasmatic nucleus (SCN). *In vitro* analyses using an embryonic rodent cell line revealed that DES was sufficient to induce *Dnmt3b* expression. Upregulating DNA methylation *in vitro* reduced expression of vasoactive intestinal polypeptide, *Vip*, and the circadian clock gene, *Bmal1*. Together, these data indicate that ovarian steroids drive *de novo* DNA methyltransferase expression in the mammalian suprachiasmatic nucleus and increased methylation may regulate genes involved in the circadian timing of oestrous: *Vip* and *Bmal1*. Overall, epigenetically mediated neuroendocrine reproductive events may reflect an evolutionarily ancient process involved in the timing of female fertility.

Key words: Rhythmic epigenetics, circadian, neuroendocrine, oestrogen

Total Words: 7331; Figures: 5; Supplementary Materials: Figure (1) Table (3)

Introduction

Gonadotropin-releasing hormone (GnRH) is an evolutionarily conserved neuropeptide that is necessary for sexual reproduction (1). In mammals, the oestrous cycle is characterized by gonadotropin pulses that exhibit low frequency during the luteal phase but increase significantly during the follicular phase (2). On the evening of proestrous, there is a circadian-dependent surge in gonadotropin secretion; after which GnRH pulse frequency slows considerably (3). A fundamental feature of the circadian timing of the proestrous surge is a neural network between the suprachiasmatic nucleus (SCN) and the anterior hypothalamus/preoptic area (AH/POA) (4). Multiple SCN neurons provide tissue-level control for timing the luteinizing hormone (LH) surge. Two neuropeptides highly expressed in the SCN that are consistently implicated in driving GnRH release include vasoactive intestinal polypeptide (*Vip*) (5) and arginine vasopressin (*Avp*) (6).

There is now strong evidence that epigenetic modifications affect the timing of puberty (7,8), but whether epigenetic modifications are involved in the neuroendocrine control of the oestrous cycle remains uncharacterized. DNA methylation is one type of epigenetic modification present in diverse taxa and is involved in the control of gene regulation (9); normally associated with transcriptional silencing. DNA methyltransferases (*Dnmt*) are a family of enzymes that catalyse the transfer of methyl-groups to the genome template (10) to maintain the pattern of methylation (imprinting control) or to modify the methylation pattern *de novo*. It has recently emerged that *de novo* DNA methylation is reversible and can exhibit clear oscillations in post-mitotic cells (14). In mammals *de novo* methylation activity is performed primarily by two Dnmt3 enzymes, Dnmt3a and Dnmt3b, encoded by separate genes (11, 12). Dnmt3a and Dnmt3b can induce both CpG and non-CpG methylation and exhibit similar kinetic activity (11). Both Dnmt3a and Dnmt3b express multiple distinct isoforms with some that lack DNA methylation activity (i.e. *Dnmt3b3,* see 11). Dnmt3a and Dnmt3b show highly conserved expression patterns across mammalian evolution with high expression in brain and reproductive tissues (e.g. testes and uterus) (12,13). It has recently emerged that *de novo* DNA methylation is reversible and can exhibit clear oscillations in post-mitotic cells (14). In uterine tissue, expression of Dnmt3a and Dnmt3b in endometrial cells (15-17) appears to be involved with decidualization (18). The prevailing hypothesis is that Dnmt3a-driven changes in uterine function is a critical step for synchronising peripheral reproductive function in mammals (15,16). In the brain, *de novo* DNA methyltransferase expression has been localized in several hypothalamic nuclei, including diencephalic centres

critically involved in reproduction, such as the SCN (19,20), the ependymal layer along the 3rd ventricle (3rdV) (21) and the AH/POA (22).

Siberian hamsters are an important animal model for studying the neuroendocrine control of reproductive physiology (23,24). Prior work in hamsters demonstrated that hypothalamic global DNA methylation was elevated in long-day breeding compared to short-day reproductively regressed hamsters (21). Increased global DNA methylation in the hypothalamus correlated with significantly higher *Dnmt1* and *Dnmt3a* expression (25). Seasonal variation in hypothalamic *Dnmt3a* expression has also been associated with photoperiod induced changes in the timing of seasonal physiology and migratory behaviour in the red-headed bunting (*Emberiza bruniceps*) (26). Seasonal changes in hypothalamic *Dnmt3a/b* expression also correlates with increased methylation in the proximal promoter of a thyroid hormone deiodinase gene (*Dio3*) (21) and is negatively correlated with *Dio3* expression (21,26). These data indicate that rhythmic epigenetic modifications, such as neuroendocrine variation in DNA methylation, is associated with the long-term programming of seasonal reproduction (14).

The objectives of the current study were to examine anatomically localised changes and ovarian-steroid dependent regulation of *de novo* DNA methyltransferase expression in the female hypothalamus. Using Siberian hamsters, we investigated *Dnmt3a* and *Dnmt3b* mRNA during proestrous and oestrous to understand if expression changes prior to -or after the LH surge. Then, we ovariectomised females and administered either a single bolus injection of oil or an ovarian steroid mixture of the highly potent estrogen agonist diesthylstilbestrol (DES) and progesterone (P) compared to vehicle control to identify hormone-dependent effects on Dnmt3a and Dnmt3b protein expression in the hamster hypothalamus. Next, we cultured a rodent embryonic cell line derived from mouse hypothalamus (mHypoE N36/1) to explore the ability of DES to regulate the expression of *Dnmt3a* and *Dnmt3b in vitro.* We also tested the impact of DES administration on the expression of neuropeptides implicated in timing the gonadotropin surge during proestrous, including *Vip*, vasopressin (*Avp*) and kisspeptin (*Kiss1*). To identify a functional role of DNA methylation for timing reproductive physiology, we then used the mHypoE N36/1 cells to investigate whether epigenetic modifying drugs influence the expression of *Vip, Avp* and *Kiss1*. Furthermore, we examined the impact of increased DNA methylation on circadian clock genes: brain and muscle ARNT-like 1 (*Bmal1*), period 1 (*Per1*) and clock (*Clock*). Our findings suggest that ovarian steroids control the expression of *de novo* DNA methyltransferases in distinct regions

of the hypothalamus and increased DNA methylation may influence multiple genomic targets involved in the neuroendocrine regulation of the oestrous cycle.

Methods

Siberian hamster colony and ethical approvals

These studies used female hamsters derived from a colony maintained at the University of Aberdeen. Hamsters were housed in polypropylene cages illuminated for 16h/day (lights-on 800h). Harlan food and tap water were provided *ad libitum* and each cage was provided cotton-nesting material. All procedures were approved by the University of Aberdeen Animal Welfare and Ethics Committee and Home Office (PPL 70/7017). All procedures were in accordance with the Arrive Guidelines for ethical research involving animals.

Study 1 – Characterization of *Dnmt3a* and *Dnmt3b* expression during the hamster proestrous and oestrous stages

Animals:

Adult female (3-8 months, n=19) were taken from the University of Aberdeen breeding colony and group housed. Animals were kept in LD (16L:8D) and samples were collected between 1500h-1700h to capture the proestrous surge in prolactin (15, 27). The age range of female hamsters was equivalent across both experimental groups. Hamsters were then sacrificed using cervical dislocation and brains were collected and frozen on powdered dry ice before being transferred to -70°C. The reproductive state of the hamsters was published previously (15). We investigated RNA expression in hypothalami from proestrous (n=11) and oestrous (n=8) hamsters.

Anatomical localization and dissection of the Siberian hamster anterior hypothalamus

Brains were placed ventral side facing upward into a cold mouse brain matrix (Alto matrix; CellPoint Scientific). The Allen Mouse atlas was used to determine the anatomical localization of an anterior tissue punch that included the SCN, anteroventral-periventricular (AvPv) and POA, and a posterior punch that comprised the arcuate nucleus (Arc) and dorsalmedial hypothalamus (DMH). The posterior extent of the optic chiasm provided a reliable anatomical landmark to separate the anterior-posterior hypothalamic divide. A second coronal section was performed 1mm in the anterior direction (AH) and a 2mm coronal section in the posterior direction (PH). Tissue sections were then placed on a cold microscope slide, the lateral and dorsal extent of the

hypothalamus was identified, and cuts conducted to isolate the respective hypothalamic regions (Figure S1).

RNA extraction, cDNA synthesis and quantitative PCR (*qPCR) assay*

AH and PH hypothalamic tissue punches were homogenized in Trizol (ThermoFisher Scientific) and RNA extracted as per manufacturer's guidelines. RNA concentration and the 260/280 ratio were measured by NanoDrop (ThermoFisher Scientific). cDNA synthesis was carried out using First Strand cDNA synthesis kit (Invitrogen). To measure mRNA expression, cDNA was assayed using qPCR run on a BioRad CFX96. For each well the qPCR mix consisted of 5µl cDNA template, 10µl SYBR green (PrecisionPLUS qPCR Master Mix with SYBR green) 0.5µl (300nM) forward primer, 0.5µl (300nM) reverse primer and 4µl RNase-free H2O to make up to 20µl. Primers were all ordered from Invitrogen, sequences for *Gnrh*, *Rfrp3*, *Kiss1*, *Dnmt1*, *Dnmt3a*, and *Dnmt3b* were optimized and published previously (21, 28) as well and the primer sequences for the reference genes glyceraldehyde 3-phosphate dehydrogenase (*Gapdh*) and hypoxanthine phosphoribosyltransferase 1 (*Hprt*) (15) (Table S1). Melt curve analyses were carried out to ensure specificity for each reaction. PCR Miner (29) was used to determine reaction efficiencies (E) and quantification cycle (Cq). According to MIQE guidelines, samples with efficiency values below 0.8 and above 1.2 were excluded from analyses (30). Fold expression of each target gene was measured in relation to the geometric mean of the Cq for two reference genes (*Gapdh* and *Hprt*) and calculated using 2-(ΔΔCq). The geometric average of the reference genes was stably expression across groups [CT $\bar{x}$±SEM Est (15.4±0.2) and Pro (15.5±0.1)].

Study 2: Assessment of ovarian steroids on Dnmt3a and Dnmt3b expression in the female hamster hypothalamus.

Animals:

Adult female hamsters (n=18) were ovariectomised and maintained in LD (16L:8D) for 8 weeks to allow circulating ovarian hormones to clear from the circulation. In brief, ovariectomies were conducted while hamsters were under deep anaesthesia (5% isofluorane gas). The ovaries were externalized via bilateral incisions to the dorsum (lateral to the spine, caudal to the ribcage). The ovary was localized at the distal end of the uterine horn and ligated with sterile sutures (4–0, nonabsorbable monofilament nylon). The ovary was then excised and the procedure was repeated for the second ovary. The abdominal wall and skin were closed separately with sterile sutures.

Hamsters recovered under analgesia and had *ad libitum* access to enriched food (sunflower seeds additional standard chow) and water before being transferred back to individual cages. 8 weeks following surgery a reduction in body mass of 7.5g (± 0.9g SEM) on average was observed and a reliable indicator of reduced ovarian steroids (31) and were previously reported (see 15). Hamsters were then randomly allocated into two experimental groups, one group to receive vehicle control (i.e. vegetable oil) and the other to receive an ovarian steroid injection. Diethylstilbestrol (DES, Sigma-Aldrich) is a highly potent estrogen agonist (E_2) with full activity at both the estrogen receptor-α and -β and was administered in conjunction with progesterone (P_4, Sigma-Aldrich). DES and P_4 (denoted as E_2P_4) were dissolved in sterile vegetable oil (Oil) to a final dose of 50µg E_2 and 5mg P_4 per ml vegetable oil. These steroid concentrations were taken from previous work in female hamsters (32). Control hamsters (n=7) were injected with 100µl oil and treatment hamsters (n=11) were injected with 100µl E_2P_4 cocktail (5µg E_2 and 500µg P_4) at 1700h. Female hamster were killed by cervical dislocation either 12- or 24-hours post-injection and the brain were rapidly extracted and frozen in dry ice.

Anatomical localization of Dnmt3a and Dnmt3b expression in the female hypothalami

Brains were then transferred to -70°C until tissue section. Brains were coronally sectioned at 30µm thickness on a cryostat (Leica 3050 series) and mounted onto poly-L-lysine/gelatine coated slides. Sections were taken from the anterior commissure through to the caudal aspect of the 3rdV, the full dorso-ventral extension of the hippocampal pyramidal layer was used as an anatomical marker for hypothalamic localization. Coronal sections were grouped into sets (each set consisted of every 8th section) spanning the entire extent of the hypothalamus. By sectioning in this manner, we were able to encompass the rostrally located POA, SCN, 3rdV and the caudally located Arc. Tissue sectioned slides were stored at -70°C until histological assays.

Immunohistochemistry

Immunohistochemistry (IHC) was carried out on slide mounted coronal brain sections. The IHC protocol started with a 10-minute fixation step in ice cold 4% paraformaldehyde followed by three washes in 0.1M phosphate buffered saline (PBS) for 5mins each. Antigen retrieval was carried out using 10mM sodium citrate pH 6.0 (Sigma-Aldrich) heated to 95°C for 20mins then after three washes in PBS, slides were incubated in 3% H_2O_2 (Fisher Scientific) for 30mins at room temperature. Serum blocking was carried out using a species appropriate serum (either goat

or horse serum, Vector labs) at 5% in PBS for 1hr at room temperature. Slides were again washed using PBSt (0.1M PBS + 0.1% Triton-X (Sigma-Aldrich)) before being incubated with primary antibody diluted in 5% serum at the optimised concentration (see Table S2) at 4°C for 48hrs. After 3 PBSt washes, sections were incubated with a biotinylated secondary antibody appropriate for the species that the primary antibody was raised in for 1hr at room temperature. In this study, the Tyramide Signal Amplification (TSA) Biotin system was used to amplify the signal (Perkin-Elmer, NEL700A001) (33). Briefly, once slides had been incubated with the respective biotinylated secondary antibody, they were washed in PBSt and then incubated with streptavidin-horseradish peroxidase conjugate for 30mins at room temperature. Slides were then washed in PBSt 3 times for 5mins, and subsequently incubated with tyramide solution for 7mins at room temperature. Slides are washed with PBSt before incubation with avidin-conjugated fluorescein (A-2001, Vector Labs) for 1hr in a darkened room. Slides were then washed in H_2O for 5mins, then cover slipped with DAPI (H-1200, Vector Labs).

The human peptide used to generate the Dnmt3a antibody (catalogue no. 3598; Cell Signalling Technologies, UK) shares 100% sequence homology with the hamster Dnmt3a sequence, whereas an epitope-tagged recombinant mouse Dnmt3b protein was used to generate the Dnmt3b antibody (52A1018; Novus Biologicals, UK) which shares 94% sequence homology to the characterised hamster sequence. Moreover, the antibody has been shown to exhibit cross species reactivity with sheep, rat and humans. We included multiple negative controls in our IHC protocol, including omitting primary antibody, omitting secondary antibody, or omitting TSA amplification to test for non-specific signal generation. In all cases, negligible immunoreactive signal was generated. Pre-adsorption controls were conducted for Dnmt3a using a Dnmt3a blocking peptide (3227BP-50 Cambridge Bioscience). Pre-adsorption controls used 1/500 primary antibody and either 1/100, 1/250 or 1/500 blocking peptide concentrations for 3 hours before incubation with hamster tissue. All sections with blocking peptide had the Dnmt3a immunoreactive signal eliminated.

Mapping and analyses of hypothalamic Dnmt3a and Dnmt3b immunoreactivity

Images were captured using Axiovert 200M (Zeiss) inverted fluorescent microscope with the Axiovison (version 4.7) software and Hammamatsu camera. Image analysis was carried out using ImageJ software (http://imagej.nih.gov/ij/) with the Fiji bioimaging plugin (34). Photomicrograph images were collected and used to measure immunoreactive Dnmt3a (ir-

Dnmt3a) and Dnmt3b (ir-Dnmt3b) cell numbers and signal intensity. Overall, ir-Dnmt3a had a diffuse distribution in the hypothalamus with higher expression levels in the SCN and Arc. The Allen mouse atlas was used as a guide to determine the borders of the SCN, Arc and POA. The ventral and medial boundaries of the SCN and Arc were determined by the base of the hypothalamus and 3rdV, respectively. The expression of ir-Dnmt3a and ir-Dnmt3b cells in the SCN and Arc were within the dorsal and lateral boundaries outlined in the Allen mouse atlas. ir-Dnmt3b stain was localised to the ependymal layer of the 3rdV and SCN. Sections were approximately 240µm apart as recommended by West (35) for stereological counting of cells. Positively stained cells were counted using the Cell Counter plug-in integrated in the Fiji package where only the leading edge of positively stained cells were counted. Images were converted to 8-bit greyscale, then each cell was circled using the circle selection tool on Fiji and the mean greyscale measured. For each section 3, background measurements (adjacent brain region without positive cells) were taken to determine non-specific background fluorescence. The background was then subtracted from fluorescence intensity of each cell to allow for normalised signal intensities to be compared across images. Immunoreactive positive cell counts and signal intensity was measured for ir-Dnmt3a in the SCN and Arc, and ir-Dnmt3b in the SCN and 3rdV.

Study 3 - *in vitro* analyses of DES and hyper- and hypo-DNA methylation on neuropeptides, circadian clock genes and *de novo* DNA methyltransferase expression.

Cell culture

The mHypoE N36/1 neuronal cell line, derived from an embryonic mouse hypothalamus (36) was used to examine the impact of hyper-methylation and Dnmt inhibition in conjunction with hormonal regulation of mRNA levels. The mHypoE N36/1 neuronal line was selected as these cells provide an optimal *in vitro* model to complement the hypothalamic oestrous analyses conducted in Study 1. Furthermore, as *de novo* DNA methyltransferase enzymes are expressed across multiple hypothalamic nuclei (19-22); these cells provide a model to identify the effect of DES and hyper- and hypo-DNA methylation agents on select neuroendocrine targets. Cells were grown in a humidified incubator at 37°C in 5% CO_2 in Dulbeccos Modified Eagle Media (DMEM - high glucose; 4,500mg/L glucose, L-glutamine and sodium bicarbonate (D5796, Sigma-aldrich), supplemented with fetal bovine serum (FBS, 10%, ATCC), penicillin (10units/ml), and streptomycin (10µg/ml) (Pen/Strep 100x, ThermoFisher) in T75 flasks (FisherScientific). Cells grown to 80% confluency before passage with trypsin/EDTA (ThermoFisher) then split and

reseeded into a clean T75 flask. mHypoE N36/1 cells were used for a maximum of 25 total passages after which fresh cells were revived from frozen stocks. For experiments, cells were trypsinised and resuspended in growth media to quantify cell density and viability using trypan blue and a haemocytometer. Cells were seeded at a density of $5x10^5$ cells/well in growth media in 24-well plates (Corning) and allowed to adhere and grow for 24 hr in a humidified incubator.

The treatment groups were divided across 4 experiments. In the hypermethylation experiment, cells were exposed to 3mM 3-aminobenzamide (3AB, Sigma-Aldrich) or vehicle control (DMSO). 3AB is a well-characterized drug that induces hyper-methylation via the inhibition of poly(ADP-ribosyl)ation (37) and has previously been shown to increase hypothalamic DNA methylation in hamsters (21). In the Dnmt inhibition experiment, cells were incubated with 100μM zebularine (ZEB, Selleckchem) or control (saline). We examined *Kiss1*, *Avp* and *Vip* expression in response to 3AB and ZEB as these neuropeptides are involved in the control of reproductive physiology and previously shown to be regulated by DNA methylation (38-40). To test the influence of ovarian steroids, cells were incubated with 1nM diethylstilbesterol (DES, Sigma-Aldrich) or vehicle control (ethanol). Finally, a hormone positive control experiment was run using cells exposed to 10mM dihydrotestosterone (DHT, Sigma-Aldrich), or ethanol (vehicle control). Prior to hormone treatments, cells were subjected to serum starvation for 24hr using serum-free growth media, followed by a saline wash. Serum-free media was used for DES and DHT experiments to minimize any confounding effects of serum steroid hormones (41). Cells used in the 3AB, ZEB and DTH experiments were incubated with 1ml of respective treatment media for either 9hr or 24hrs in a humidified chamber with 5% CO_2 at 37°C. Cells treated with DES were incubated with 1ml of respective media for only 24hrs. All samples were lysed *in vitro* using RLT buffer supplemented with 1% v/v β-mercaptoethanol from the Qiagen RNeasy Mini kit and stored at -70°C.

RNA extraction and cDNA synthesis

RNA from cells was isolated using the RNeasy Mini Kit (Qiagen). According to the manufacturer's protocol using 33ul nuclease-free H2) to elute the purified RNA from the spin column. The concentration of eluted RNA was determined using a NanoDrop (ThermoFisher) and the RNA was then stored at -70°C until further processing. cDNA was synthesized using oligo dT primers (Precision nanoScript2 Reverse Transcription kit, Primer Design) according to the manufacturer's directions.

qPCR assay for Dnmt3a, Dnmt3b and reproductive neuropeptides

qPCRs were run on a BioRad CFX96 Real time PCR machine in a 20µl reaction. Primers were supplied by Invitrogen and the primer sequences are provided in Table S3. Both *Dnmt3a* and *Dnmt3b* express multiple isoforms in many human, mouse and rat tissues. The hamster *Dnmt3a* and *Dnmt3b* primers are not designed to distinguish between the various *Dnmt3a* and *Dnmt3b* isoforms described in rodents (i.e. mice or rats). Therefore, the qPCRs for *Dnmt3a* and *Dnmt3b* provide an overall assessment of transcript levels. All samples were run in duplicate in a 96-well plate format under the following cycling conditions; i) initial denaturing at 95°C for 5min, then 39 cycles of ii) 95°C for 10secs, iii) 30 secs at annealing temperature dependent on gene of interest, then iv) an extension step of 72°C for 30secs. For each qPCR assay no-template H_2O controls (NTC) were included. Melt curve were examined to confirm specificity of the amplification reaction. PCR Miner (25) was used to determine reaction efficiencies (E) and quantification cycle (Cq). According to MIQE guidelines, samples with efficiency values below 0.8 and above 1.2 were excluded from analyses (30). Fold expression of each target gene was measured in relation to the geometric mean of the Cq for two reference genes (*gapdh* and *βactin*) and calculated using 2-(ΔΔCq). The reference gene was stable across treatment groups and drug treatments [CT $\bar{x}$±SEM Control (19.6±0.1) and 3AB (19.5±0.1); [CT $\bar{x}$±SEM Control (22.1±0.1) and DES (22.1±0.1)]; and [CT $\bar{x}$±SEM Control (17.9±0.2) and ZEB (18.2±0.7)].

Statistical analyses

For Study 1, a two-tailed t-test was conducted to determine whether the expression of hypothalamic *Dnmt1*, *Dnmt3a* and *Dnmt3b* was different between proestrous and oestrous females. Since *Dnmt3a* expression increased during oestrous, we conducted one-tailed t-tests to examine statistical significance in the E2P4 driven changes in the number of ir-Dnmt3a and ir-Dnmt3b cells and signal intensity. Moreover, one-tailed t-tests were also conducted on DES-driven mRNA expression in Study 3. Data were log-transformed in the event a violation of normality was observed. Statistical analyses were performed using SigmaPlot 13.0 and significance was determined at $p \leq 0.05$.

Results

Hypothalamic *Dnmt3a* expression varies between proestrous and oestrous stages

The precision of the tissue punches targeting the AH and PH was confirmed by *Gnrh, Kiss1* and *Rfrp3* mRNA expression. *Gnrh* was only identified in the AH, *Kiss1* was localized to the AH (i.e. AvPv/POA) and PH (i.e. Arc), and *Rfrp3* was expressed at higher levels in the PH (i.e. DMH) (Fig S1C-E). *Dnmt3a* expression was significantly higher in the AH tissue-punches during oestrous ($P<0.05$), but neither *Dnmt1* ($P>0.20$) nor *Dnmt3b* ($P>0.34$) differed between these stages (Fig. 1). *Dnmt1, Dnmt3a* and *Dnmt3b* expression in the PH did not vary across the oestrous stages ($P>0.05$ for all comparisons). *Dnmt3a* expression was significantly higher in the AH, whereas *Dnmt1* and *Dnmt3b* expression was significantly greater in the PH (data not shown).

Ovarian steroids stimulate ir-Dnmt3a and ir-Dnmt3b in hypothalamic nuclei.

To determine the impact of ovarian steroids, adult hamsters were ovariectomized (OVX) and after 8 weeks were treated with E_2P_4 or vehicle control (oil), and ir-Dnmt3a/b immunoreactivity was examined histologically either 12h or 24h later. There was no significant effect of time on ir-Dnmt3a nor ir-Dnmt3b expression in any nuclei examined ($P>0.18$ for all comparisons). Therefore, we combined the data from both treatment groups. E_2P_4 was found to significantly increase the number of ir-Dnmt3a cells in the SCN (Fig. 2A-B; $P=0.05$), without influencing their fluorescence intensity (Fig. 3A; $P>0.05$). In the Arc, ir-Dnmt3a cell numbers were not affected by E_2P_4 (Fig. 2C-D; $P>0.05$), nor was their fluorescence intensity (Fig. 3B; $P>0.05$). Furthermore, E_2P_4 treatment failed to alter the number of ir-Dnmt3b cells or signal intensity in the 3rdV (Fig. 2E-F, Fig. 3D, respectively; $P>0.49$), but caused an increase in ir-Dnmt3b signal intensity in the SCN (Fig. 3C; $P<0.05$). Collectively, these data indicate that ovarian steroids markedly upregulate ir-Dnmt3a and ir-Dnmt3b expression specifically in the SCN. When compared to the oestrous study data, these results indicate that *de novo* DNA methyltransferase expression in anterior hypothalamic tissues including the SCN changes over the course of the female ovarian cycle; increased *Dnmt3a* expression coincides with, and is likely driven by, elevated ovarian steroid secretion.

The potent estrogen analogue DES upregulates *Dnmt3b* expression *in vitro.*

In order to begin to elucidate the molecular mechanisms by which ovarian hormones affect DNA methyltransferase activity in the HPG axis, we sought to develop a tractable *in vitro* model. To accomplish this, we used a well-characterised cell model, the embryonic mouse hypothalamic cell line, mHypoE N36/1 (36) to test whether DES would influence *Dnmt3a* and *Dnmt3b*

expression and alter the expression of reproductive neuropeptides. Following incubation with DES, *Kiss1* ($P=0.01$) and *Vip* ($P<0.05$; Fig. 4A) were significantly downregulated in mHypoE N36/1 cells, whereas there was no effect on *Avp* expression ($P>0.14$). *Dnmt3b* expression was significantly upregulated in DES treated cells ($P<0.05$; Fig. 4B), but DES failed to alter *Dnmt1* ($P>0.19$) or *Dnmt3a* ($P>0.36$) expression. Collectively, these results indicate that DES signalling via estrogen receptor upregulates *Dnmt3b* expression, without significantly affecting *Dnmt1* or *Dnmt3a* expression, pointing to a degree of specificity in the effects of ovarian hormone secretion on *de novo* DNA methyltransferase induction.

This assay was also used to examine whether *Dnmt3a/b* expression can be induced in response to the non-aromatizable androgen, dihydrotestosterone (DHT), which would offer insights into whether, *in vivo*, effects of DES on *Dnmt3a* and *Dnmt3b* can be mediated via androgen receptors. DHT failed to induce *Dnmt1, 3a* or *3b* expression as compared to vehicle treated controls (Fig. 4C; $P>0.10$, all comparisons), indicating that, in this paradigm, androgens are not sufficient to upregulate *Dnmt* expression, and may indicate that, *in vivo*, estrogen signalling may be the essential pathway by which gonadal hormones activate hypothalamic *Dnmt* expression.

Functional role of DNA methylation on neuropeptide and circadian clock genes

In order to identify potential targets of increased hypothalamic DNA methylation, we used two epigenetic-modifying drugs to either inhibit Dnmt enzymes with ZEB or hyper-methylate DNA using 3AB. Treatments did not affect transcript expression across 9- and 24-hr sampling points ($P>0.28$); therefore we collapsed the data to simplify the presentation of the results. To eliminate any potential effects of time on clock gene expression; qPCR was conducted using cells treated with 3AB for 24hrs. We identified 2 genes expressed in the SCN that were significantly reduced after exposure to 3AB, *Vip* (Fig 5A; $P<0.05$) and *Bmal1* (Fig 5B; $P<0.05$). The 3AB-induced hypermethylation appears to be specific as no differences in expression other reproductive neuropeptides gene (i.e. *Kiss1, Avp*) (Fig. 5A; $P>0.16$) or other circadian clock genes (i.e. *Per1, Clock*) (Fig. 5B; $P>0.27$) were observed. However, ZEB treatment reduced DNA methyltransferase but did not significantly alter *Vip*, *Kiss1,* or *Avp* expression (Fig. 5C; $P>0.28$). The lack of an effect may be due to the relatively short exposure of the cells to ZEB (i.e. <24hrs).

Discussion

While the impact of epigenetic modifications has been implicated in timing fertility in peripheral tissues (15-17), a role in the hypothalamus has not been investigated. This study examined the distribution of *Dnmt3a* and *Dnmt3b* across the hamster oestrous cycle and identified that ovarian steroids stimulate ir-Dnmt3a and ir-Dnmt3b expression in the SCN. During proestrus, AH (i.e. SCN) *Dnmt3a* expression is significantly reduced; this effect was anatomically specific, as no effect was observed in the PH, which is also sensitive to ovarian steroid feedback. Together these data reveal a novel neuroendocrine mechanism in which epigenetic modifications driven by DNA methylation in the SCN control fertility timing in mammals. We propose that DNA methylation in the SCN provides transient inhibition on critical genes (i.e. *Vip, Bmal1*) that in turn, promotes cyclic changes in fertility and female sexual behaviour which constitute the oestrous cycle.

These data indicate that DNA methylation may regulate SCN gene transcription as females transition from proestrous to the oestrous stage. *Vip* is highly expressed in the SCN and is critical for the synchronization and maintenance of molecular timekeeping (42). VIP immunoreactive neurons in the SCN also project directly onto GnRH neurons, with greater abundance after puberty (43). Male and female *Vipr2*$^{-/-}$ mice exhibit reduced fertility, and females exhibit irregular oestrous cycles (44), consistent with a model in which *Vip*, localized in the core circadian nuclei, functions as an integral part of the molecular machinery, regulating the neuroendocrine output of GnRH neurons. Here, we extend this model to indicate that *Vip* expression is significantly reduced by DES, and this may be mediated by the increased expression of *Dnmt3a/3b* driven DNA methylation. DES was sufficient to stimulate the expression of *Dnmt3b* mRNA; whereas DES and progesterone was required to drive Dnmt3a protein expression. Given the observation that Dnmt3a and Dnmt3b have dissociable effects on the genome (45), it is likely that ovarian steroids exerted independent effects on DNA methylation by selectively recruiting different Dnmt3a/b enzymes throughout the oestrous cycle. Furthermore, as the levels of estrogen receptor-α and -β expression are very low in the SCN (46), it is likely that ovarian steroids act in other hypothalamic nuclei (e.g. Arc, 47) and indirectly regulate *de novo* DNA methyltransferase expression in the SCN. Further examination of how estrogen and progesterone signalling regulate SCN *dnmt3a* and *dnmt3b* expression is warranted.

The daily control of female reproductive physiology requires kisspeptin-dependent regulation of GnRH release (2,5, 48). Avp-expressing cells in the SCN project to Kiss1 neurons in the anteroventral periventricular and periventricular preoptic nuclei (AvPv/PeN) and may provide

SCN-dependent circadian timing of oestrous (6). 3AB hypermethylation of mHypoE N36/1 cells did not affect *Avp* nor *Kiss1* expression. These findings suggest that *de novo* DNA methylation may not be involved in the hamster SCN Avp to AvPv/PeN kisspeptin to GnRH neuroendocrine pathway. However, further research using *in vivo* approaches are required to determine whether DNA methylation regulates either Avp or kisspeptin signalling across the oestrous cycle.

One pathway through which this novel effect may be mediated is via the circadian clock gene *bmal1*, which is a core component of the circadian clock, and is also a target for Dnmt3a (49). *In vitro* hyper-methylation via 3AB reduced *Bmal1* expression within 24 hrs and thus indicates a functional role of DNA methylation induced changes in circadian clock gene transcription. The lack of an effect on other circadian clock genes (i.e. *Per1*) is likely due to the single 24hr sampling period. The assessment of circadian clock gene expression over several days is necessary in order to determine the downstream effect of increased DNA methylation on the *Bmal1* expression. Daily DNA methylation oscillations in the *Bmal1* promoter likely exerts a critical role on the oestrous cycle by maintaining the functional integrity of the circadian transcriptional-translational feedback loop, which regulates the timing of the luteinizing hormone surge during proestrous. The present data here add to a growing body of work which indicates that, beyond its well-characterised role in embryogenesis and gametogenesis**,** rhythmic *de novo* methylation may be widespread in the adult brain.

Rhythmic changes in *de novo* DNA methyltransferase enzymes across seasonal time scales have been reported in the hypothalamus (21,25,27), gonads (15), liver (50) and leukocytes (51). The evidence indicates that *Dnmt3a* and *Dnmt3b* expression are regulated by a combination of environmental and endogenous signals (52). The present study reveals anatomically localized effects of ovarian steroids on *Dnmt3a* and *Dnmt3b* expression and indicates that rhythmic DNA methylation might be a novel component for the timing of female fertility. The availability of the Siberian hamster genome will facilitate the dissection of localized rhythmic DNA methylation across neuroendocrine and peripheral reproductive tissues (53).

References

1. Stevenson TJ, MacDougall-Shackleton SA, Hahn TP, Ball GF. Gonadotropin-releasing hormone plasticity: a comparative perspective. Front. Neuroendocrinol. 2012; 33:287-300.
2. Herbison AE. The gonadotropin-releasing hormone pulse generator. Endocrinol. 2018; 159:3723-3736.

3. McQuillan HJ, Han SY, Cheong I, Herbison AE. GnRH pulse generator activity across the estrous cycle of female mice. Endocrinol. 2019; *in press.*
4. Herbison AE. Multimodal influence of estrogen upon gonadotropin-releasing hormone neurons. Endocr. Rev. 1998; 19:302-330.
5. Williams WP, Kriegsfeld LJ. Circadian control of neuroendocrine circuits regulating female reproductive function. Front. Endocrinol. 2012; 3:60.
6. Vida B, Deli L, Hrabovszky E, Kalamatianos T, Caraty A, Coen CW, Liosits Z, Kallo I. Evidence for suprachiasmatic vasopressin neurones innervating kisspeptin neurones in the rostral periventricular area in the mouse brain: regulation by oestrogen. J. Neuroendocrinol. 2010; 22:1032-1039.
7. Lomniczi A, Ojeda SR. The emerging role of epigenetics in the regulation of female puberty. Endocr. Dev. 2016; 29:1-16.
8. Lomniczi A Wright H, Ojeda RS. Epigenetic regulation of female puberty. Front. Neuroendocrinol. 2015; 36:90-107.
9. Law JA, Jacobsen SE. Establishing, maintaining and modifying DNA methylation patterns in plants and animals. Nat. Rev. Genet. 2010; 11:204-220.
10. Lyko F. The DNA methyltransferase family: a versatile toolkit for epigenetic regulation. Nat. Rev. Genet. 2018; 19:81-92.
11. Aoki A, Suetake I, Miyagawa J, Fujio T, Chijiwa T, Sasaki H, Tajima S. Enzymatic properties of *de novo* type mouse DNA (cytosine-5) methyltransferases. Nucl. Acids Res. 2001; 29:3506-3512.
12. Sakai Y, Suetake I, Shinozake F, Yamashina S, Tajima S. Co-expression of de novo DNA methyltransferases Dnmt3a2 and Dnmt3L in gonocytes of mouse embryos. Gen Exp Patt. 2004; 5:231-237.
13. Coyle CS, Tolla E, Stevenson TJ. Rhythmic epigenetics in neuroendocrine and immune systems. In *Developmental Neuroendocrinology* eds Wray S & Blackshaw S. Springer, New York. 2019.
14. Stevenson TJ. Epigenetic regulation of biological rhythms: an evolutionary ancient molecular timer. Trend Genet. 2018; 43:90-100.
15. Lynch EWJ, Coyle CS, Lorgen M, Campbell E, Bowman A, Stevenson TJ. Cyclical DNA methyltransferase 3a expression is a seasonal and oestrus timer in reproductive tissues. Endocrinol. 2016; 157:2469-2478.

16. Roy A, Matzuk MM. Deconstructing mammalian reproduction: using knockouts to define fertility pathways. Reproduction 2006; 131:207-219.
17. Van Kaam KJ, Delvoux B, Romano A, D'Hooghe T, Dunselman GA, Groothuis PG. Deoxyribonucleic acid methyltransferase and methyl-CpG binding domain proteins in human endometrium and endometriosis. Fertil. Steril. 2011; 95:1421-1427.
18. Logan PC, Ponnampalam AP, Steiner M, Mitchell MD. Effect of cyclic AMP and estrogen/progesterone on the transcription of DNA methyltransferase during the decidualization of human endometrial stromal cells. Mol. Hum. Reprod. 2013; 19:302-312.
19. Azzi A, Dallmann R, Casserly A, Rehrauer H, Patrignani A, Maier B, Kramer A, Brown SA. Circadian behaviour is light-reprogrammed by plastic DNA methylation. Nat. Neurosci. 2014; 17:377-382.
20. Azzi A, Evans JA, Leise T, Myung J, Takumi T, Davidson AJ, Brown SA. Network dynamics mediate circadian clock plasticity. Neuron 2017; 2017:441-450.
21. Stevenson TJ, Prendergast BJ. Reversible DNA methylation regulates seasonal photoperiodic time measurement. Proc. Natl. Acad. Sci. 2013; 110:16651-16656.
22. Nugent BM, Wright CL, Shetty AC, Hodes GE, Lenz KM, Mahurkar A, Russo SJ, Devine SE, McCarthy MM. Brain feminization requires active repression of masculinization of DNA methylation. Nat. Neurosci. 2015; 18:690-697.
23. Stevenson TJ, Alward BA, Ebling FJP, Fernald RD, Kelly A, Ophir A. Revisiting Krogh's principle and the value of the comparative approach. Policy Insights Behav. Brain Sci. 2018; 5:118-125.
24. Lewis JE, Ebling FJP. Hamsters as a model species for neuroendocrine studies. In *Model Animals in Neuroendocrinology: from worm to mouse to man* (eds Ludwig M, Levkowitz G). Wiley Online Library. 2018; Doi.10.1002/9781118381128.ch7
25. Stevenson TJ. Circannual and circadian rhythms in hypothalamic DNA methyltransferase and histone deacetylase in Siberian hamsters (*Phodopus sungorus*). Gen. Comp. Endocrinol. 2017; 243:130-137.
26. Sharma A, Singh D, Malik S, Gupta NJ, Rani S, Kumar V. Difference in control between spring and autumn migration in birds: insight from seasonal changes in hypothalamic gene expression in captive buntings. Proc. R Soc. B. 2018; 285(1885).
27. Dodge JC, Kristal MB, Badura LL. Male induced estrus synchronization in the female Siberian hamster (*Phodopus sungorus*). Physiol. Behav. 2002; 77:227-231.

28. Banks R, Delibegovic M, Stevenson TJ. Photoperiod- and triiodothyronine-dependent regulation of reproductive neuropeptides, proinflammatory cytokines, and peripheral physiology in Siberian hamsters (*Phodopus sungorus*). J. Biol. Rhythms 2016; 31:299-307.
29. Zhao S, Fernald FD. Comprehensive algorithm for quantitative real-time polymerase chain reaction. J. Comp. Biol. 2005; 12:1047–1064.
30. Bustin SA, Benes V, Garson JA, Hellemans J, Huggett J, Kubista M, Mueller R, Nolan T, Pfaffl MW, Shipley GL, Vandesompele J, Wittwer CT. The MIQE guidelines: minimum information for publication of quantitative realtime PCR experiments. Clin. Chem. 2009; 55:611–622.
31. Bartness TJ. Wade GN. Photoperiodic control of seasonal body weight cycles in hamsters. Neurosci. Biobehav. Rev. 1985; 9:599–612.
32. Meisel RL, Luttrell VR. Estradiol increases the dendritic length of ventromedial hypothalamic neurons in female Syrian hamsters. Brain Res. Bull. 1990; 25:165-168.
33. Stevenson TJ, Calabrese MD, Ball GF. Variation in enkephalin immunoreactivity in the social behaviour network and song control system of male European starlings (*Sturnus vulgaris*) is dependent on breeding state and gonadal condition. J Chem Neuroanat. 2012; 43:87-95.
34. Schindelin J, Arganda-Carreras I, Frise E, Kaynig V, Longair M, Pietzsch T, Preibisch S, Rueden C, Saalfeld S, Schmid B, Tinevez JY, White DJ, Hartenstein V, Eliceiri K, Tomancak P, Cardona A. Figi: an open-source platform for biological-image analysis. Nat. Methods 2012; 9:676-682.
35. West MJ. Design-based stereological methods for counting neurons. Prog. Brain Res. 2002; 135:43-51.
36. Belsham DD, Cai F, Cui H, Smukler SR, Salapatek AM, Shkreta L. Generation of a phenotypic array of hypothalamic neuronal cell models to study complex neuroendocrine disorders. Endocrinol. 2004; 145:393-400.
37. Zardo G, D'Erme M, Reale A, Strom R, Perilli M, Caiafa P. Does poly(ADP-ribosyl)ation regulate the DNA methylation pattern? Biochemistry 1997; 36:7937-7943.
38. Stroud H, Su SC, Hrvatin S, Greben AW, Renthal W, Boxer LD, Nagy MA, Hochbaum DR, Kinde B, Gabel HW, Greenberg ME. Early-life gene expression in neurons modulates lasting epigenetic states. Cell 2017; 171:1151-1164.

39. Auger CJ, Coss D, Auger AP, Forbes-Lorman RM. Epigenetic control of vasopressin expression is maintained by steroid hormones in the adult male rat brain. PNAS 2011; 108:4242-4247.
40. Wyatt AK, Zavodna M, Viljoen JL, Stanton JA, Gemmell NJ, Jasoni CL. Changes in methylation patterns of kiss1 and kiss1r gene promoters across puberty. Genet Epigenet. 2013; 5:51-62.
41. Shifren JL, Tseng JF, Zaloudek CJ, Ryan IP, Meng YG, Ferrara N, Jaffe RB, Taylor RN. Ovarian steroid regulation of vascular endothelial growth factor in the human endometrium: implications for angiogenesis during the menstrual cycle and in the pathogenesis of endometriosis. J. Clin. Endo. Metabol. 1996; 81:3112-3118.
42. Maywood ES, Reddy AB, Wong GK, O'Neill JS, O'Brien JA, McMahon DG, Harmar AJ, Okamura H, Hastings MH. Synchronization and maintenance of timekeeping in suprachiasmatic circadian clock cells by neuropeptidergic signalling. Curr. Biol. 2006; 16:599-605.
43. Kriegsfeld LJ, Silver R, Gore AC, Crews D. Vasoactive intestinal polypeptide contacts on gonadotropin-releasing hormone neurones increase following puberty in female rats. J. Neuroendocrinol. 2002; 14:685-690.
44. Dolatshad H, Campbell EA, O'Hara L, Maywood ES, Hastings MH, Johnson MH. Developmental and reproductive performance in circadian mutant mice. Human Reprod. 2006; 21:68-79.
45. Auclair G, Guibert S, Bender A, Weber M. Ontogeny of CpG island methylation and specificity of DNMT3 methyltransferases during embryonic development in the mouse. Genome Biol. 2014; 15:545.
46. Shughrue PJ, Lane MV, Komm B, Merchenthaler I. Comparative distribution of estrogen receptor-α and -β mRNA in the rat central nervous system. J Comp. Neurol. 1997; 388:507-525.
47. De La Iglesia HO, Blaustein JD, Bittman EL. Oestrogen receptor-α immunoreactive neurones project to the suprachiasmatic nucleus of the female Syrian hamster. J. Neuroendocrinol. 1999; 11:481-490.
48. Simonneaux V, Piet R. Neuroendocrine pathways driving daily rhythms in the hypothalamic pituitary gonadal axis of female rodents. Curr. Opin. Physio. 2018; 5:99-108.

49. Koike N, Yoo SH, Huang HC, Kumar V, Lee C, Kim TK, Takahashi JS. Transcriptional architecture and chromatin landscape of the core circadian clock in mammals. Science 2012; 338:349-354.
50. Alvarado S, Mak T, Liu S, Storey KB, Szyf M. Dynamic changes in global and gene-specific DNA methylation during hibernation in adult thirteen-lined ground squirrels, *Ictidomys tridecemlineatus*. J Exp. Biol. 2015; 218:1878-1795.
51. Stevenson TJ, Bradley SP, Onishi KJ, Prendergast BJ. Cell-autonomous iodothyronine deiodinase expression mediates seasonal plasticity in immune function. Brain Behav. Immun. 2013; 36:61-70.
52. Stevenson TJ. Environmental and hormonal regulation of neuroendocrine epigenetic enzymes. J. Neuroendocrinol. 2017; 29(5).
53. Bao R, Onishi KG, Tolla E, Ebling FJP, Lewis JE, Anderson RL, Barrett P, Prendergast BJ, Stevenson TJ. Genome sequencing and transcriptome analyses of the Siberian hamster hypothalamus identifies novel mechanisms for seasonal energy balance. Proc. Natl. Acad. Sci. 2019; 116:13116-13121.

Figure Legends

Figure 1 – Oestrous plasticity in DNA methyltransferase mRNA expression in the anterior hypothalamus. The fold change in *Dnmt3a* mRNA in the anterior hypothalamus had significantly higher expression during oestrous (EST) compared to proestrous (PRO) hamsters. Neither *Dnmt1* nor *Dnmt3b* were observed to be significantly different between PRO and EST stages. Asterisks indicate statistical significance by * $P<0.05$. Numbers in the bar graph denote sample size.

Figure 2 – Ovarian steroids stimulate Dnmt3a in the suprachiasmatic nucleus. A single bolus injection of an estrogen analogue diethylstilbestrol (DES) and progesterone (denoted as E_2P_4) was found to have anatomically localized effects on Dnmt3a and Dnmt3b expression in the hypothalamus. Ovariectomized hamsters that received E_2P_4 significantly increased the number of Dnmt3a cells in the suprachiasmatic nucleus (SCN) compared to oil treated controls (OVX) (A). Representative photomicrographs of Dnmt3a immunoreactivity in the SCN (B). There was no effect of E_2P_4 on Dnmt3a immunoreactive cells in the Arc (C, D). There was no significant effect of E_2P_4 on Dnmt3b immunoreactive cells in the ependymal layer along the 3rdV (E, F). White lines denote the boundary of the SCN (B) and Arcuate (D). The white arrows indicate immunoreactive Dnmt3a/b cells. Abbreviations: 3rd ventricle (3rdV), Arcuate (Arc), oestrous (EST), Median eminence (ME), proestrous (PRO) and Suprachiasmatic nucleus (SCN). Asterisks indicate statistical significance by * $P<0.05$. Numbers in the bar graph denote sample size.

Figure 3 – Ovarian steroid regulation of *de novo* DNA methyltransferase immunoreactive intensity in the female hamster hypothalamus. Dnmt3a cell intensity in the SCN (A) and Arc (B) was not significantly different between ovariectomized females treated with oil or E_2P_4. Ovarian steroids were found to significantly increase Dnmt3b signal intensity in the SCN (C), but there was no significant effect on immunoreactivity in the 3rdV (D). Asterisks indicate statistical significance by * $P<0.05$. Numbers in the bar graph denote sample size.

Figure 4 – Diethylstilbestrol and Dihydrotestosterone effects on neuropeptide and DNA methyltransferase expression. Using mHypoE N36/1 (an immortalized hypothalamic neuronal cell line) neurons were treated with the highly potent estrogen agonist diethylstilbestrol (DES) (A, B). DES caused decreases in vasoactive intestinal polypeptide (*Vip*) and kisspeptin (*Kiss1*) expression (A) and upregulated *Dnmt3b* expression (B). There was no significant effect on vasopressin (*Avp*), *Dnmt1* or *Dnmt3a*. Cells treated with DHT did not show significant variation in *Dnmt1*, *Dnmt3a* or *Dnmt3b* expression (C). Asterisks indicate statistical significance by * $P<0.05$. Numbers in the bar graph denote sample size.

Figure 5 - *In vitro* analyses of DNA methylation on neuropeptides and circadian clock gene expression. Using mHypoE N36/1 neurons were treated with either the hypermethylation compound 3-aminobenzimide (3AB) or the DNMT inhibitor zebularine (ZEB). 3AB inhibited *Vip* (A) expression and *Bmal1* (B) mRNA levels, but not vaopresson (*Avp*), kisspeptin (*Kiss1*), Clock (*Clock*) or period1 (*Per1*) expression. DNMT inhibition via ZEB application did not significantly affect *Vip, Avp* or *Kiss1* expression (C). *$P<0.05$ vs. control. Numbers in the bar graph denote sample size.

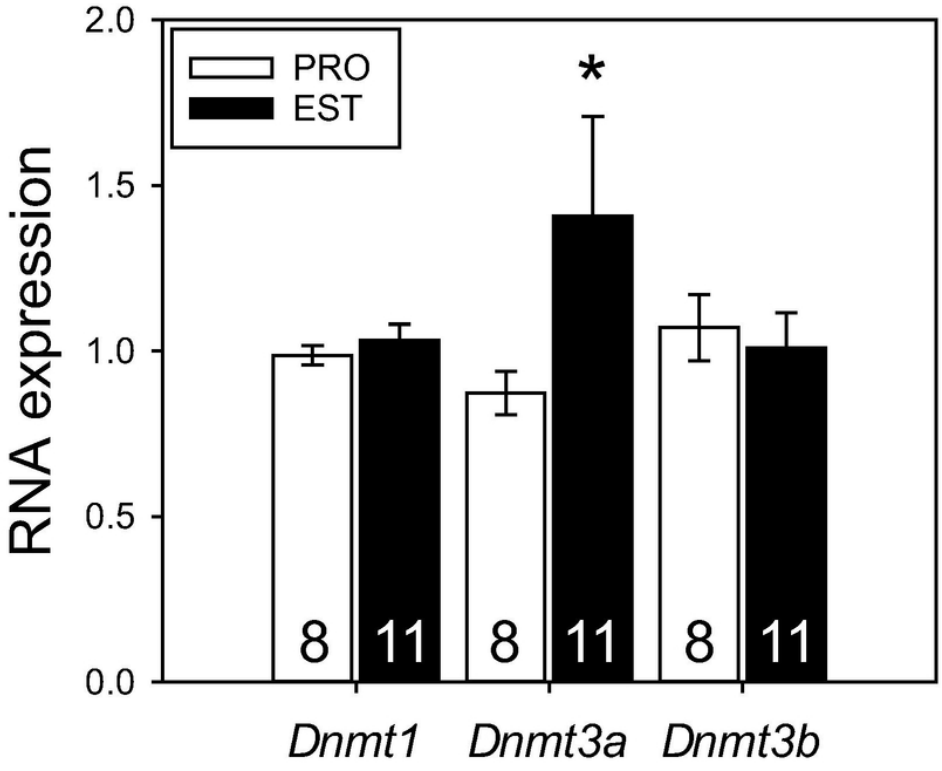
2.0
1.5
1.0
0.5
0.0
RNA expression
PRO
EST
*
8
11
8
11
8
11
Dnmt1
Dnmt3a
Dnmt3b

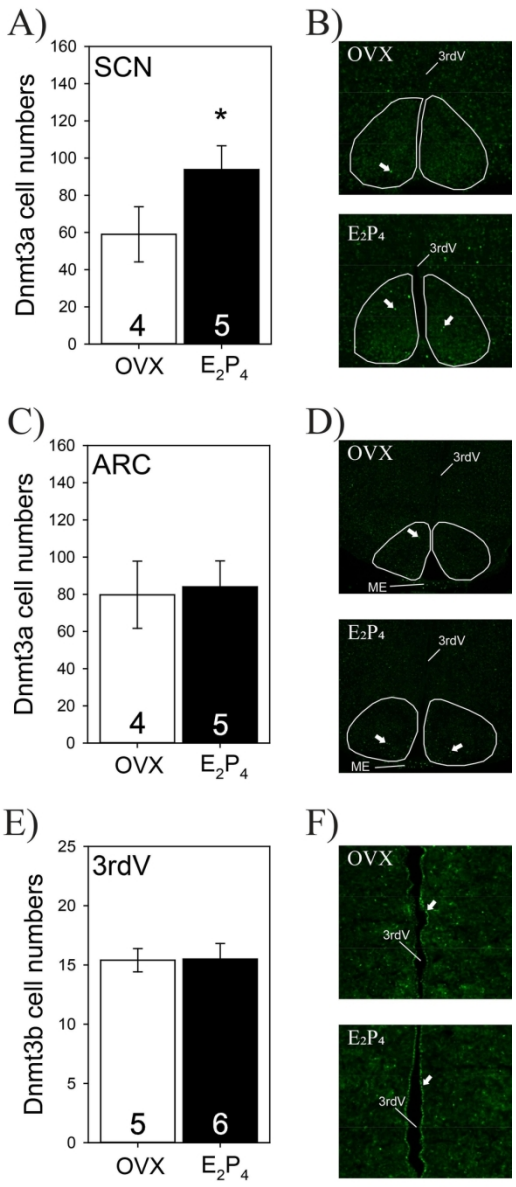
A)
SCN
Dnmt3a cell numbers
160
140
120
100
80
60
40
20
0
*
4
5
OVX
E2P4
B)
OVX
3rdV
E2P4
3rdV
C)
ARC
Dnmt3a cell numbers
4
5
OVX
E2P4
D)
OVX
3rdV
ME
E2P4
3rdV
ME
E)
3rdV
Dnmt3b cell numbers
25
20
15
10
5
0
5
6
OVX
E2P4
F)
OVX
3rdV
E2P4
3rdV

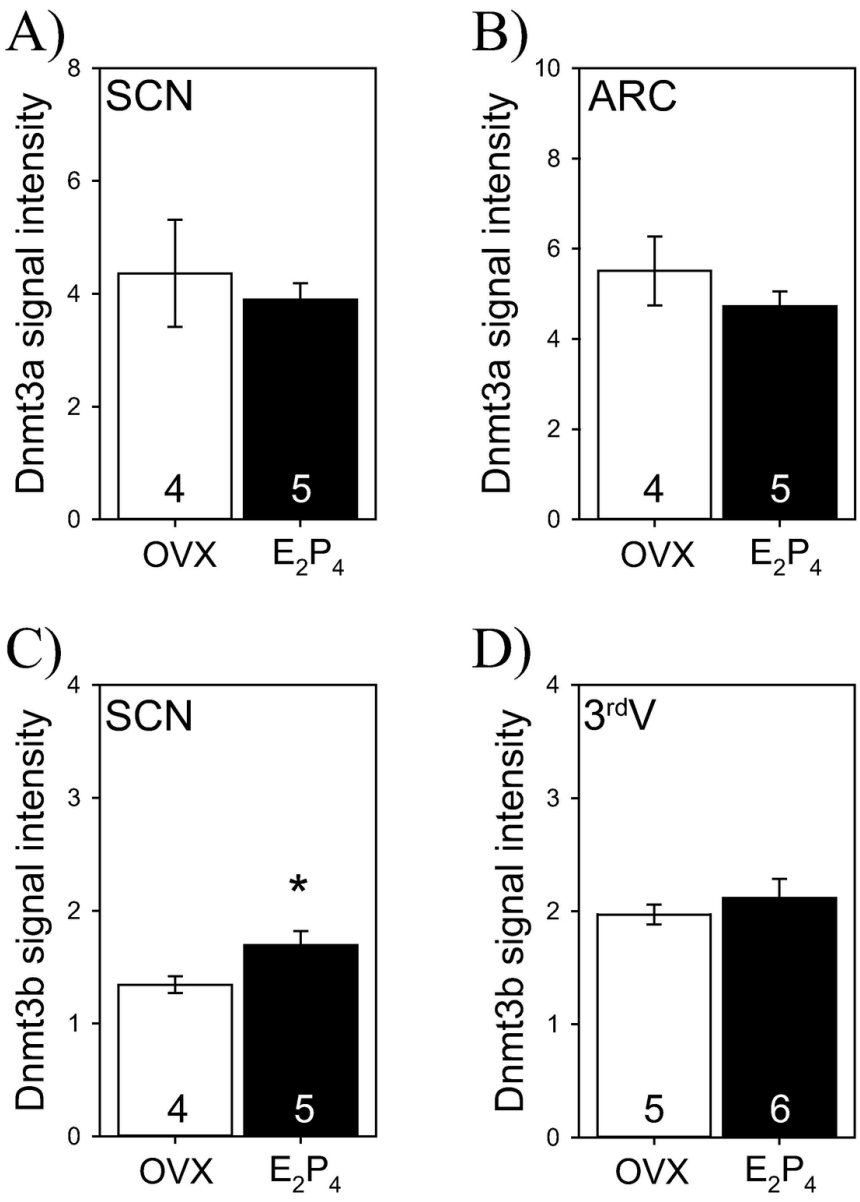

Figure 3

98x130mm (300 x 300 DPI)

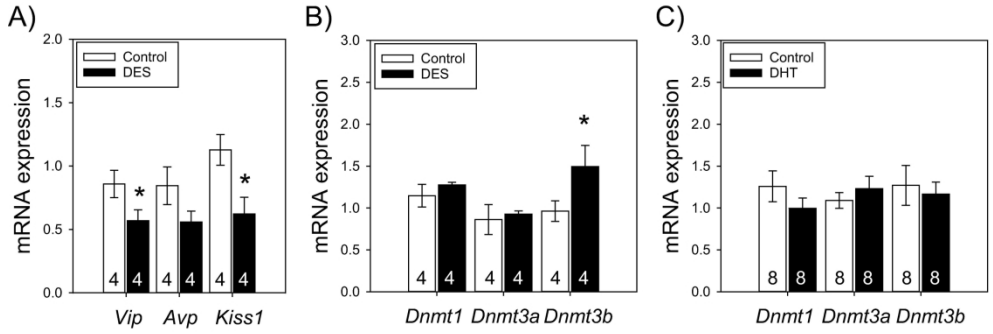
A)
B)
C)
mRNA expression
Control
DES
DHT
Vip
Avp
Kiss1
Dnmt1
Dnmt3a
Dnmt3b
*

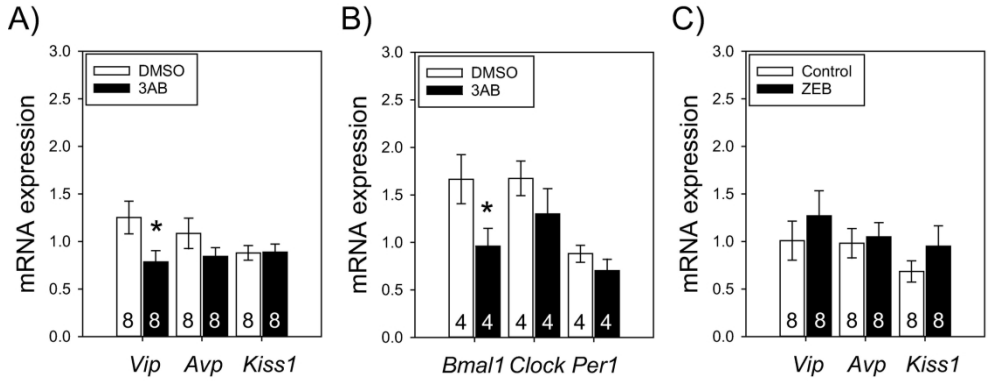
A)
B)
C)
mRNA expression
DMSO
3AB
Control
ZEB
*
8
4
Vip
Avp
Kiss1
Bmal1
Clock
Per1